Remote Sensing of Environment 281 (2022) 113236

Contents lists available at ScienceDirect

Remote Sensing of Environment

journal homepage: www.elsevier.com/locate/rse

Linking remote sensing and insect defoliation biology – A cross-system comparison

B. Thapa [a,*,1], P.T. Wolter [a], B.R. Sturtevant [b], P.A. Townsend [c]

[a] Department of Natural Resource Ecology & Management, Iowa State University, Ames, IA 50011, USA
[b] Institute for Applied Ecosystem Studies, Northern Research Station, USDA Forest Service, Rhinelander, WI 54501, USA
[c] Department of Forest and Wildlife Ecology, University of Wisconsin—Madison, 1630 Linden Drive (Suite 226), Madison, WI 53706, USA

ARTICLE INFO

Edited by Dr. Marie Weiss

Keywords:
Defoliation
Frass
Foliage loss
Spruce budworm
Jack pine budworm
Spongy moth
Landsat
Change detection

ABSTRACT

The success of space-based forest defoliation monitoring beyond thematic classification hinges on the ability to link units of continuous foliar change with associated units of spectral or vegetation index change across different systems. To explore this, we used multi-temporal Landsat sensor data with respect to three defoliation metrics (shoot-based estimates (%), frass biomass (kg·ha^{-1}), and proportion of foliar loss) across three different forest systems in the United States. While shoot-based defoliation was measured in the field, the later two defoliation metrics were estimated based on the insect phenology model, BioSIM. The systems include spruce budworm (SBW, *Choristoneura fumiferana* C). in heterogenous mixed forests, Minnesota, jack pine budworm (JPBW, *Choristoneura pinus* F). in homogenous pine forests, Wisconsin, and spongy moth (SGM, *Lymantria dispar dispar* L). in mixed broad-leaved forests, Maryland. Our generalized annual defoliation model for budworm was poor (R^2_{adj} = 0.35, RMSE = 23.70%) due to difficulty in detecting SBW defoliation in Minnesota. Thus, individual annual JPBW shoot-based defoliation models (R^2_{adj} = 0.27 to 0.75 and RMSE = 19.16% to 11.32%) outperformed the SBW models (R^2_{adj} = 0.08 to 0.27, RMSE = 23.18% to 34.13%). Cross-system differences between rates of change in ground-based metrics of defoliation with respect to observed change in spectral index values (dVI) were significant for shoot-based estimates of percent annual defoliation for SGM vs. JPBW (p-values $<1.00 \times 10^{-4}$) and SGM vs. SBW (p-values $< 4.60 \times 10^{-3}$). However, such comparison between SGM and JPBW were not significant when either frass biomass (kg·ha^{-1}, p-value = 0.46) or proportion of foliage loss was used (p-value = 0.67). For a given unit of defoliation, the magnitude of vegetation index change, dVI, was significantly different between SGM and JPBW for each defoliation metric used (p-values $<1.00 \times 10^{-4}$), but not between SGM and *SBW* (p-value = 0.47) or between JPBW and SBW (p-value = 0.06) when shoot-based annual defoliation metrics were used. This study is first to report that, for a given quantity of defoliation, substantial differences in both the magnitude and direction of vegetation index change exists for different defoliator systems, which currently precludes the development of a viable, unified defoliation model. However, outcomes of this research provide an important step in our understanding of these defoliator systems that may enable specific scaling of continuous defoliation at landscape levels and across defoliator systems in the future.

1. Introduction

Defoliating insects have pronounced effects on forest health and productivity across North America due to wide-ranging, periodic outbreaks that often persist across multiple years (Cooke et al., 2021; Dale et al., 2001; Fleming et al., 2002; Royama, 1984; Sturtevant et al., 2015; Volney and McCullough, 1994). Perhaps the most destructive and economically important insect defoliator in North America is the endemic spruce budworm (SBW, *Choristoneura fumiferana* Clem). (Volney and Fleming, 2007; Irland and McWilliams, 2014) that affected over 50 million hectares of spruce (*Picea* spp). and fir (*Abies* spp). forests in the 1970s outbreak (Sturtevant et al., 2015), which typically repeats every 35-years (Royama, 1984). Similarly, the invasive, exotic spongy moth (SGM, *Lymantria dispar dispar* L). affected over 19 million ha of eastern broadleaved forest in two consecutive outbreak cycles in 1978–1981 and 1987–1990 (Karel and Man, 2017). These extensive and

* Corresponding author.
E-mail address: btha001@iastate.edu (B. Thapa).
[1] Current affiliation: Department of Forestry and Natural Resources, Purdue University, 715 W. State Street, West Lafayette, IN 47907, USA.

https://doi.org/10.1016/j.rse.2022.113236
Received 28 February 2022; Received in revised form 19 August 2022; Accepted 22 August 2022
Available online 29 August 2022

successive years of defoliation have substantial and lasting impacts on tree growth and survival. In turn, this affects forest structure and composition (Franklin et al., 2002; Sharik et al., 2010), ecosystem function (Turner et al., 2003), nitrogen leaching (Christenson et al., 2002; Townsend et al., 2003), carbon cycle dynamics (Dymond et al., 2010), and economic losses to forest products industry (Dale et al., 2001; Karel and Man, 2017). Thus, robust methods for remote detection of biologically meaningful system impacts are critical for operational monitoring and deeper understanding of underlying insect-host dynamics (Hall et al., 2016).

Since the 1980s, the number of remote sensing studies focused on detection and mapping of insect defoliation events, and subsequent impacts, has greatly expanded, as has the sophistication of methodologies and sensors used in the process (Bhattarai et al., 2020; Donovan et al., 2021; Hall et al., 2016). However, only 67 studies (35 in broadleaved and 32 in conifer forest) focused on remote detection and mapping of insect-related forest disturbance (Thapa, 2021). Among them, 18 studies measured continuous defoliation, of which only three (all broadleaved) combined Landsat sensor data with field-measured estimates of defoliation to provide continuous estimates of percent defoliation (Hall et al., 2003; Rullán-Silva et al., 2015; Townsend et al., 2012) [Thapa, 2021]. Still, remote detection and mapping of continuous, annual defoliation of conifers beyond categorical mapping (Bhattarai et al., 2020; Donovan et al., 2021; Rahimzadeh-Bajgiran et al., 2018) remains a challenge. In addition, all of these studies were limited to either single defoliating agent (broadleaved or coniferous defoliator) or combination with intensive disturbance such as bark beetles, fire, wind or harvest (Senf et al., 2017). Here, we intend to combine both defoliators, coniferous and broadleaved to develop a single, unified defoliation model which then can be used to monitor defoliation at regional scale (Senf et al., 2017).

Tree growth reduction and mortality are each functions of cumulative defoliation, modified by host taxonomic life history traits (Foster, 2017). It generally takes several consecutive years of moderate to severe defoliation to kill host trees. Coniferous hosts are generally more sensitive to defoliation than broad-leaf species (Schowalter et al., 1986), as they experience greater growth reduction and mortality, which tends to scale positively with leaf longevity (Foster, 2017). Methods for quantifying the impact of annual or multi-year defoliation events vary greatly. Such methods may include assessments of the proportion of canopy consumed (Townsend et al., 2012), relative growth reduction (Chen et al., 2017; Kulman et al., 1963; MacLean, 1990; Pothier et al., 2005), the amount of top-kill (Hall et al., 1998; Prebble, 1975), and mortality (Chen et al., 2017; Hall et al., 1998; Howse, 1983; MacLean and Piene, 1995). Moreover, there can be substantial lag times between outbreak initiation and subsequent host mortality. For instance, it can take five to 10 years of sustained SBW infestation to kill host trees (Batzer and Hastings, 1981; Dymond et al., 2010; Fleming et al., 2002; MacLean, 1980; Robert et al., 2018). Nevertheless, if cumulative defoliation of a given host species can be reliably mapped from space via remote sensing, then the impacts on host trees may be estimated from available empirical functions (Foster, 2017).

Forest defoliator species can differ substantially in their foraging habitat and host specificity (Castagneyrol et al., 2014), which can affect remote detection (Hall et al., 2016). For instance, when populations are high, generalist broad-leaf defoliators such as SGM–prefers oak (*Quercus* spp).—and forest tent caterpillar (*Malacosoma disstria* Hübner) –prefers aspen (*Populus* spp).—will feed vigorously on the foliage of nearly all other broadleaved species, while conifer-feeding budworm species are more selective. Spruce budworm, for example, feeds mainly on the current-year foliage of four conifer species, including balsam fir (*Abies balsamea*), white spruce (*Picea glauca*), red spruce (*Picea rubens*) and black spruce (*Picea mariana*), often leaving older needles undisturbed (Leckie and Ostaff, 1988). Similarly, jack pine budworm (JPBW, *Choristoneura pinus* Freeman) feeds on pollen cones and current-year foliage of jack pine (*Pinus banksiana*), leaving two and three year old live needles intact (McCullough, 2000).

In addition, the interactions among defoliator feeding biology, tree species diversity, and system responses can complicate defoliation mapping across systems, where the word 'system' refers to different defoliators and their specific forest habitat. For instance, 100% defoliation in broadleaf systems generally translates to total removal of all foliage during the insect outbreak, which enables highly successful satellite-based disturbance mapping in such systems (Townsend et al., 2012). However, re-foliation of broad-leaf species later in the growing season of the same year of defoliation (Schowalter et al., 1986) can limit the window of opportunity for optimal remote detection (de Beurs and Townsend, 2008). In contrast, severe defoliation for conifer-feeding budworm systems (described above) generally equates to the removal of ca. 70% of the current-year's foliage (Bhattarai et al., 2020). As such, older live needles from previous growing seasons generally remain undisturbed, except for the heaviest defoliation years where "back-feeding" on older foliage may occur (Leckie and Ostaff, 1988; Rahimzadeh-Bajgiran et al., 2018). Thematic mapping of annual (e.g., none, light, moderate, and severe classes) and cumulative SBW defoliation via satellite sensor data have been successful within eastern Maritime spruce-fir forests, particularly within forests containing high host concentration (Amos-Binks et al., 2010; Bhattarai et al., 2020; Donovan et al., 2021; Rahimzadeh-Bajgiran et al., 2018). Coniferous foliar retention also varies among host species. For example, balsam fir may hold four to six years of live needles (Clark, 1961; Fleming and Piene, 1992; Reich et al., 2014), white and black spruce may retain five to 10 years of live needles (Reich et al., 2014), while jack pine typically retains only two to three years of live needles (Kulman et al., 1963; O'Neil, 1962). Therefore, the salient remote sensing challenge in these coniferous forest-insect systems is to distinguish continuous, as opposed to thematic, annual defoliation (Bhattarai et al., 2020; Donovan et al., 2021) from cumulative defoliation (Lottering et al., 2019), where host species may hold combinations of unconsumed current-year foliage plus multiple years of relatively undisturbed older live needles (Hall et al., 2016). Further, both host species concentration and relative canopy position can vary greatly across different forest-defoliator systems. All of the above complexities complicate the development of generalizable satellite-based metrics of forest defoliation impacts.

Remote sensing offers the ability to regularly quantify biological processes across complex landscapes where different disturbance agents may exhibit common manifestations such as defoliation. The goal of this study was to calibrate different ground-to-satellite defoliation models to explore potential relationships between the annual change in moderate spatial resolution Landsat sensor data (30 m) and canopy defoliation across three forest-insect systems: mixed broad-leaved forests of western Maryland impacted by SGM, homogeneous jack pine forests impacted by JPBW in northwestern Wisconsin, and heterogeneous mixed forests affected by SBW in northern Minnesota. Ultimately, we seek to identify whether the biological impacts of defoliation across different systems may be generalized and modeled using a common, satellite-based predictor. Of these systems, we expected SGM defoliation to be most intuitive and readily mapped via satellite sensor data due to SGM's generalist broadleaf diet (de Beurs and Townsend, 2008). We anticipated SBW defoliation to be the most challenging to map using satellite sensor data due to the combination of host's canopy position, multi-year needle longevity, and tree species diversity within the study region (Bhattarai et al., 2020; Franklin et al., 2008; Thapa et al., 2020). Given these two remote detection extremes, we posited that JPBW defoliation detection would represent intermediate difficulty due to unique biophysical conditions of the jack pine host, including high host concentration, dominant vertical canopy position, and relatively short needle longevity compared to SBW.

To date, satellite-based defoliation detection studies have focused on individual systems (Bhattarai et al., 2020; Radeloff et al., 1999a; Rahimzadeh-Bajgiran et al., 2018; Townsend et al., 2012) or comparisons with other severe forest disturbances, such as harvest or mortality.

In such cases, various methods are used that apply threshold values to categorically separate non-defoliated, defoliated, and harvested forest (Kennedy et al., 2010; Meigs et al., 2011; Senf et al., 2015; Zhu et al., 2012). Here, we leveraged field defoliation data from three different systems to provide quantitative inferences on continuous canopy defoliation detection for forest health monitoring and ecosystem impact assessment. More specifically, we evaluated budworm system (SBW and JPBW) defoliation models in detail and then integrated budworm data with SGM data from a prior, independent study to evaluate the degree to which a unified, cross-system model of defoliation may be possible. Canopy defoliation metrics include shoot-based estimates of defoliation (a.k.a. annual defoliation, %), frass biomass ($kg{\cdot}ha^{-1}$, caterpillar excrement), and foliage loss (proportion of foliage biomass consumed by defoliator to the total amount of foliar biomass available). While percent annual defoliation is commonly used for forest health monitoring (Donovan et al., 2021; Hall et al., 2016) and previous studies of defoliation mapping, frass biomass and foliage loss are rare in the literature to measure defoliation impacts on forest ecosystems (Dymond et al., 2010; Hicke et al., 2012; Townsend et al., 2004). Hence, this study is first to compare three different defoliation metrics to annual change in a Landsat-based vegetation index. Furthermore, our modeled estimates of frass biomass and foliage loss can be used to assess nutrient fluxes (Townsend et al., 2004) and carbon dynamics (Hicke et al., 2012), respectively, at landscape levels.

2. Study area

2.1. Northeast, Minnesota

The spruce budworm study area is located in Itasca, St. Louis, and Koochiching counties of north central Minnesota (Fig. 1). Predominant landforms in this region include glacial moraines, small outwash plains, and lake plains punctuated by ericaceous wetlands and bogs (Host and White, 2003). Dominant broadleaf tree species in the study area include quaking aspen (*Populus tremuloides*), often in mixture with paper birch (*Betula papyrifera*), and northern hardwoods such as red and sugar maple (*Acer rubrum*, *A. saccharum*) on richer soils to the south. Conifer species include jack and red pine (*P. banksiana and P. resinosa,* respectively) on excessively drained soils, while white spruce (*P. glauca*) and balsam fir (*A. balsamea*) exist on more mesic sites and are the primary SBW host in the study area. The extensive peatlands within the study area sustain stands of black spruce (*P. mariana*) and eastern larch (*Larix larcinia*). White spruce sometimes occurs in pure plantations that are specifically concentrated in the southwestern part of the study area. SBW host species, especially balsam fir, are often restricted to the understory and sub canopy of natural stands due to the unusually high frequency of SBW outbreaks (Frelich, 2002; Robert et al., 2012). A localized outbreak of approximately 110,000 ha was active across the study area at the time of field sampling (Thapa, 2021).

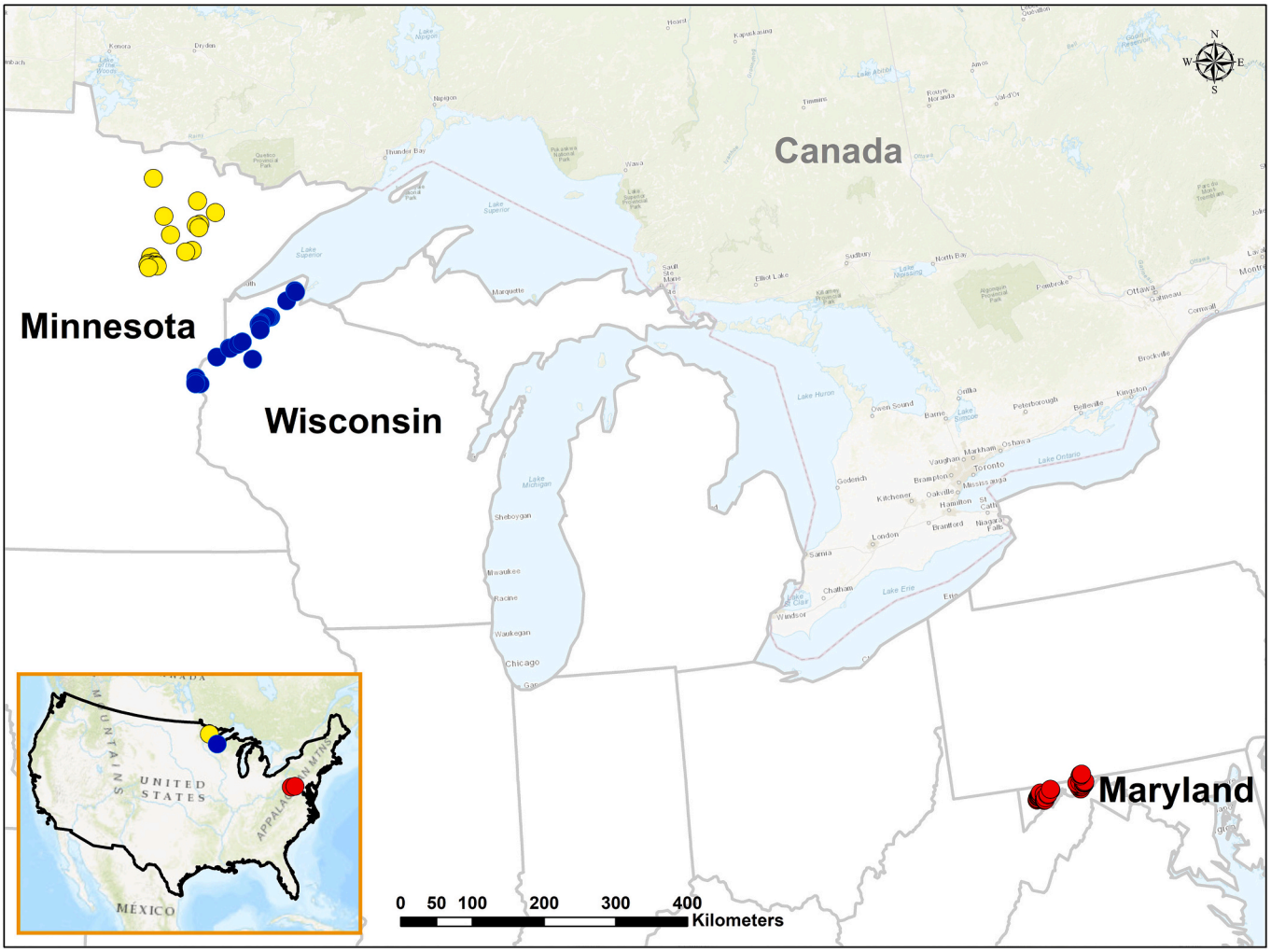

Fig. 1. Location of study sites and plots within the United States for spruce budworm (*C. fumiferana*) in Minnesota (yellow), jack pine budworm (*C. pinus*) in Wisconsin (blue) and spongy moth (*L. dispar dispar*) in Maryland (red). (For interpretation of the references to colour in this figure legend, the reader is referred to the web version of this article).

2.2. Northwest Sands, Wisconsin

The jack pine budworm study area coincides with the boundary of the Northwest Sands Ecological Landscape in northwestern Wisconsin (Fig. 1), which is a large, sandy glacial outwash region covered by a mixture of dry forests, open barrens, and agriculture (Wisconsin Department of Natural Resources, 2015). Dry forests are primarily dominated by jack pine (*P. banksiana*), but also include aspen (*Populus* spp). and scrub oak (primarily *Q. ellipsoidalis* and *Q. rubra*) in pure stands and in mixtures with jack pine (Radeloff et al., 1999b). Reforestation efforts composed of pure jack and red pine (*P. banksiana* and *P. resinosa*) plantations starting in the late 1930s increased the susceptibility of this landscape to JPBW outbreaks (Clancy et al., 1980; Vogl, 1964; Weber, 1995). The last JPBW outbreak in this area occurred from 2004 to 2007, which resulted in over 100,000 ha of defoliation (Thapa, 2021).

2.3. Western Maryland

The spongy moth study area in western Maryland (Fig. 1) consists of two state forests: Green Ridge State Forest (GR) and Savage River State Forest (SR) (see Townsend et al., 2012). The SR State Forest is located on the Appalachian Plateau, with elevations ranging between 375 and 900 m and receiving 114–140 cm precipitation annually, while GR is located in the rain shadow of the Appalachian Plateau in the Ridge and Valley physiographic province, with elevations ranging from 150 to 370 m and receiving 76-88 cm precipitation annually (Sturtevant and Seagle, 2004). The current distribution and dominance of oak species (*Quercus* spp). at both state forests is a product of frequent fires both before and after the European settlement (Mash, 1996; Shumway et al., 2001; Tyndall, 2015). Nonetheless, SR forest composition is best characterized as Appalachian mesophytic hardwood, including other broadleaf species such as maple (*Acer* spp). and black cherry (*Prunus serotina*) as well as eastern hemlock (*Tsuga canadensis*). The GR forest composition is more strongly dominated by oak and hickory (*Carya spp*), with maple in protected coves and pines (e.g., *Pinus virginianus*) on dry slopes and ridges (Sturtevant and Seagle, 2004). Since 1983, periodic SGM outbreaks affect both the GR and SR sites. The last severe defoliation from SGM occurred between 2000 and 2001 in GR and between 2006 and 2008 in SR (Townsend et al., 2012; Thapa, 2021).

3. Materials and methods

3.1. Field data

Field plots consisted of five variable radius subplots within which the authors collected and recorded defoliation data in all field sites during outbreak years. A factor-two metric prism was used to estimate forest basal area ($m^2 \cdot ha^{-1}$) by species from 2005 to 2006, 2003 to 2004, and 2000 to 2008 at the Wisconsin, Minnesota and Maryland sites, respectively (Appendix A, Table S1–1). Randomly selected host trees within each plot were measured (DBH, cm) and used to estimate dry foliar biomass ($kg \cdot ha^{-1}$) according to allometric equations from Jenkins et al. (2003) for the Maryland sites and Ter-Mikaelian and Korzukhin (1997) for the Wisconsin sites, henceforth referred to simply as foliage biomass.

Among the three different metrics of defoliation (Appendix A, Table S1–2), annual defoliation (%) and frass biomass ($kg \cdot ha^{-1}$) were collected during the field survey. We leveraged our weekly frass data to estimate the actual amount of foliage consumed based on the "approximate digestibility" of host foliage from published laboratory experiments for each respective defoliator (Barbosa and Greenblatt, 1979; Carisey and Bauce, 1997). We then added weekly green fall deposition data (foliage dislodged but not consumed) to our calculated ingested foliar biomass vales ($kg \cdot ha^{-1}$) to derive the total amount of foliar biomass ($kg \cdot ha^{-1}$) removed. Defoliator- and location-specific food consumption phenology models (BioSIM, Régnière, 1996) were used to backfill data, according to Thapa et al. (2022), when and where deposition windows were missed during field sampling campaigns. We summed weekly frass and the total amount of foliar biomass removed by seasons to estimate cumulative annual frass and foliar biomass, respectively. Finally, the proportion of foliage loss (range: 0–1, where one is equivalent to 100% loss of foliage biomass), hereafter referred to as foliage loss, was calculated as the ratio of cumulative annual foliar biomass removed to available foliar biomass, which was calculated from tree diameter data via allometric equations (as discussed above). Note that while frass and green fall data were collected for the SBW system, we found the deposition within dense, mixed forests to be highly variable, which precluded reliable frass-based estimation of defoliation (B. Sturtevant, personal observation). Hence, we didn't analyze frass or frass-derived data for SBW in this study.

In addition to frass, traditional metrics of percent annual defoliation were also measured within each study area. We followed Volney (1992) for JPBW and MacLean and MacKinnon (1998) for SBW to sample host trees, where we followed the Fettes shoot count method (Fettes, 1950) on individual host trees to estimate both percent annual defoliation (a.k.a., current-year defoliation) on current-year foliage and the previous year's foliage (range: 0% - 100). With respect to SGM defoliation at the SR and GR sites, we visually assessed defoliation percent in situ (range: 0% - 100%) for 66 field plots every week for the entire 2006, 2007 and 2008 field seasons and then weighted these visual estimates by DBH according to Townsend et al. (2012). The JPBW and SBW ground plots that clearly experienced forest management activity such as salvage logging (Radeloff et al., 2000) (visually assessed via historic Google Earth imagery) and aerial pesticide spraying since the initial 2004 sampling season were removed from our analyses.

3.2. Landsat data

We acquired cloud free atmosphere- and terrain-corrected Landsat-5 Thematic Mapper (TM) and Landsat-7 Enhance Thematic Mapper Plus (ETM+) satellite sensor data (see Masek et al., 2006; Vermote et al., 1997) from the United States Geological Survey (USGS) via the Earth Explorer portal (https://earthexplorer.usgs.gov/) (Appendix B, Table S2–1,Appendix C, Tables S3 1–3). Landsat image selection criteria for change detection analyses included several factors: finding near anniversary dates from year to year, minimizing date-wise differences in atmospheric relative humidity (< 10%), and use of images with similar solar elevation angles (< 10°) to mitigate canopy shading differences. For images collected in the winter season, we excluded images recorded following recent snowfall events (< two weeks) or images dates that did not experience wind speeds in excess of 25 $km \cdot h^{-1}$ following older snowfall events to ensure that host canopies would be free of snow.

Problems and limitation associated with the use of summer imagery to detect budworm defoliation are well documented (e.g., Bhattarai et al., 2020; Ekstrand, 1990, 1994; Leckie, 1987). Hence, we evaluated Landsat-based vegetation indices from different seasons (i.e., winter, early, and growing) to test the sensitivity of change in vegetation index with respect to canopy defoliation. Vegetation indices include normalized difference vegetation index (NDVI), moisture stress index (MSI), normalized difference infrared index (NDII), middle infrared index (MIR) and shortwave to visible ration (SVR5) (Appendix B, Table S2–2). We used the Random Forest (RF) routine (v.4.6–14, Breiman, 2001) within R (R Core Team, 2013) to evaluate sensitivity of vegetation index and season against current-year JPBW defoliation data (Appendix B). Our preliminary efforts suggested that difference in NDVI derived from winter Landsat sensor data were good predictors of annual JPBW defoliation. Therefore, we used winter NDVI for SBW defoliation detection, as the two defoliators have similar feeding traits and life history.

The winter season provides other optical advantages relevant to budworm defoliation detection. During the winter following a defoliation event, defoliated shoots are often more exposed to space-based sensors, as well as any budworm-damaged cells and pigments in the

remaining live foliage (sensu Rock et al., 1988). These factors affect overall forest reflectance via an increase in visible red reflectance combined with a proportional decrease in NIR reflectance (Leckie et al., 1988; Rock et al., 1988), which serves to drive forest NDVI values down. In addition, lower sun elevation angles (typical in winter at ca. 47.5° N Lat). are preferred for detecting budworm defoliation damage using Landsat sensor data (Ekstrand, 1990). Under winter's low sun elevation conditions (e.g., 28 °), understory forest layers are largely shaded. Thus, these lower forest layers have a diminished effect on overall canopy reflectance, while the illuminated upper canopy's budworm damage signal is likely bolstered (Ekstrand, 1990). Hence, we used Landsat-based NDVI from winter seasons for budworm defoliation detection (JPBW and SBW) and NDII from the summer growing season for spongy moth (Townsend et al., 2012).

3.3. Change detection in budworm systems

We applied a commonly used bi-temporal (pre- and post-disturbance) change detection method (Coppin et al., 2004) to detect defoliation induced by budworm and spongy moth using Landsat-based vegetation indices. As described above, we used different vegetation indices (VI) from different seasons for the budworm and spongy moth systems. To simplify vegetation index abbreviations, hereafter we refer to the selected vegetation index as VI and the corresponding vegetation index difference images as dVI. In addition, our primary interest was to detect annual defoliation via annual changes in the respective VIs, regardless of initial defoliation condition and outbreak stage. Using each of the respective VIs, we used the generalized equation below (Eq. 1) to calculate VI differences to enhance defoliation detection, where subscript *Y* represents a pre-disturbance year and subscript *Y + 1* represents a post-disturbance year.

$$dVI = VI_{Y+1} - VI_{Y} \quad (1)$$

In this study, a pre-disturbance year is a year before the disturbance event regardless of insect outbreak year or forest condition. For example, we used respective VIs from 2004, 2005, and 2006 as pre-disturbance years for annual defoliation for 2005, 2006, and 2007, respectively.

Finally, we evaluated selected Landsat sensor data for potential confounding effects from topography, WRS-2 path-related view angle geometry, sun elevation angle (Claverie et al., 2015; Roy et al., 2016; Song and Woodcock, 2003), and relative humidity (Rosas et al., 2017) on resulting shoot-based estimates of annual defoliation (Appendix C, Fig. S3–2). Hence, we applied a standardized l2-normalization procedure (Goodfellow et al., 2017) to minimize potential effects of aforementioned sources. These effects were a concern for our study because we used data from both the Landsat-5 and -7 sensors and, in some cases, sensor data from neighboring WRS-2 path overlap areas (i.e., P26–27), which have very different view angle geometries for common forest targets. Thus, we sampled pixels in WRS-2 path overlap areas (P26 and P27) within reflectance-stable red-pine stands (dark dense vegetation, DDV) in Wisconsin and Minnesota to assess potential path-wise effects on NDVI values (Appendix C, Text S1, Tables S3–4-5, Figs. S3–1, see detail). Because index values resulting from the l2-normalizaiton were all less than approximately 4×10^{-5}, we standardized these output values to fit the range of NDVI (−1 to 1) (Appendix C).

3.4. Data analysis

Informed by our initial qualitative, exploratory analysis of ground and satellite data scatterplots (Appendix C, Fig. S3–2), we used linear models to fit annual budworm defoliation (JPBW and SBW) field data to annual change in NDVI from winter image. Then, we combined dNDII data for SGM (Townsend et al., 2012) and wdNDVI data for budworm (SBW, JPBW) to test linear and non-linear regression models to fit vegetation index change, dVI, to our respective field defoliation data. For example, we tested non-linear sigmoid models (Eq. 2); where *a* is the asymptote, *b* is the rate of change parameter, c is the midpoint of dVI at which slope is maximum, and dVI is the difference in vegetation index.

$$Defoliation = \frac{a}{1 + exp(b^{*}(dVI - c))} \quad (2)$$

In addition, we evaluated the effects of different sample years and defoliators by using a mixed-effects model. Then, we selected the optimal model based on Akaike's Information Criterion (AIC, (Sakamoto et al., 1986)), root mean square error (RMSE), and delta AIC (delta AIC > 2; (Burnham and Inference, 2002)). Accuracy of models was assessed using one of the cross-validation methods such as Leave-one-out cross validation for model development, K-year cross validation for budworm-specific annual defoliation model, bootstrapping, and simulation of the model for calculation of 95% confidence interval of RMSE. In addition, we used second derivative analysis of the non-linear sigmoid model (Eq. 2) to determine the inflection point at which change in defoliation with respect to dVI is significant.

4. Results

4.1. Annual defoliation in budworm systems (SBW and JPBW)

Annual JPBW defoliation models for individual years performed moderately well compared to the relatively poor results for the SBW models (the range of R^2_{adj} and RMSE values for JPBW vs. SBW, respectively, are 0.27–0.75 vs. 0.08–0.27 and 11.29%–17.74% vs. 24.06%–34.32%, Table 1, Fig. 2). This result remained consistent when annual defoliation data across three years were pooled to develop budworm-specific defoliation models (R^2_{adj} = 0.52 vs. 0.14 and RMSE = 15.44 vs. 30.46% for JPBW vs SBW [Table 1]). Thus, K-year cross-validation results for each budworm-specific defoliation model were consistent, with average RMSE values of 15.47% for JPBW and 32.33% for SBW (Table 2). In addition, the use of sample year as a covariate did not significantly affect the rate of change in dVI with respect to defoliation (respective JPBW and SBW *p*-values were 0.22 and 0.35). However, the SBW model intercept indicated that the magnitude of change in dVI was significantly different between sample years (*p*-value = 0.03). Further exploration of the intercepts among SBW models revealed that dVI difference between the 2005 and 2006 defoliation years was significant (*p*-value = 0.04).

In addition to model differences by year, we explored whether SBW defoliation models were sensitive to forest structural parameters, such as species composition, host basal area, or naturally occurring host versus plantations. Our forest structural differences analyses did not reveal any substantial effects on our ability to detect defoliation using dVI (Appendix D, Figs. S4–1-2). Likewise, we did not see any clear patterns between USFS aerial sketch maps, field measurements, and dVI (Appendix D, Figs. S4–3-4).

Finally, we combined annual defoliation data from all sample years and both budworm systems (JPBW and SBW) to develop one, cross-system, global model for budworm (*Choristoneura*) defoliation. We found that the model that included budworm type (JPBW, SBW) as a covariate was optimal (R^2_{adj} = 0.35, RMSE = 23.70%, Table 3, Fig. 3). Similar to the budworm-specific models described above, the sample year covariate did not significantly affect the model performance (*p*-value = 0.43). Further analysis of the global model revealed that the intercepts for two budworm systems were significantly different (*p*-value $<4.53 \times 10^{-3}$), while the slopes were not significantly different (*p*-value = 0.45). However, exploratory removal of plots that had <10% annual defoliation suggested that the respective intercept and slope values between the JPBW and SBW models were not significantly different (*p-values*: 0.36 for intercept, 0.24 for slope).

Table 1
Annual defoliation model results for each individual year and combined years for each defoliator: jack pine budworm and spruce budworm. Winter normalized difference vegetation index (NDVI) imagery from pre- and post-defoliation years (yr) were used to calculate the difference in vegetation index (dVI). Model performance metrics reported here include adjusted R^2 (R^2_{adj}), root mean square error (RMSE), AIC, *p*-value, and leave-one-out cross-validation (LOOCV): RMSE and mean absolute error (MAE).

Defoliators	Model description	Model				LOOCV		
		DF	R^2_{adj}	RMSE	AIC	*p*-value	RMSE	MAE
Jack pine budworm	Defoliation ~ dVI [yr = 2004]	13	0.53	17.74	132.70	1.26×10^{-3}	19.16	15.73
	Defoliation ~ dVI [yr = 2005]	21	0.27	14.93	193.53	6.20×10^{-3}	16.90	13.98
	Defoliation ~ dVI [yr = 2006]	19	0.75	11.29	165.28	1.92×10^{-7}	11.32	9.42
	Defoliation ~ dVI	57	0.52	15.44	494.36	4.42×10^{-11}	15.59	12.40
Spruce budworm	Defoliation ~ dVI [yr = 2004]	13	0.08	34.32	152.49	0.15	34.13	29.17
	Defoliation ~ dVI [yr = 2005]	20	0.15	29.14	214.71	0.15	28.64	23.34
	Defoliation ~ dVI [yr = 2006]	14	0.27	24.06	151.04	0.02	23.18	19.29
	Defoliation ~ dVI	51	0.14	30.46	516.51	2.57×10^{-3}	30.97	26.71

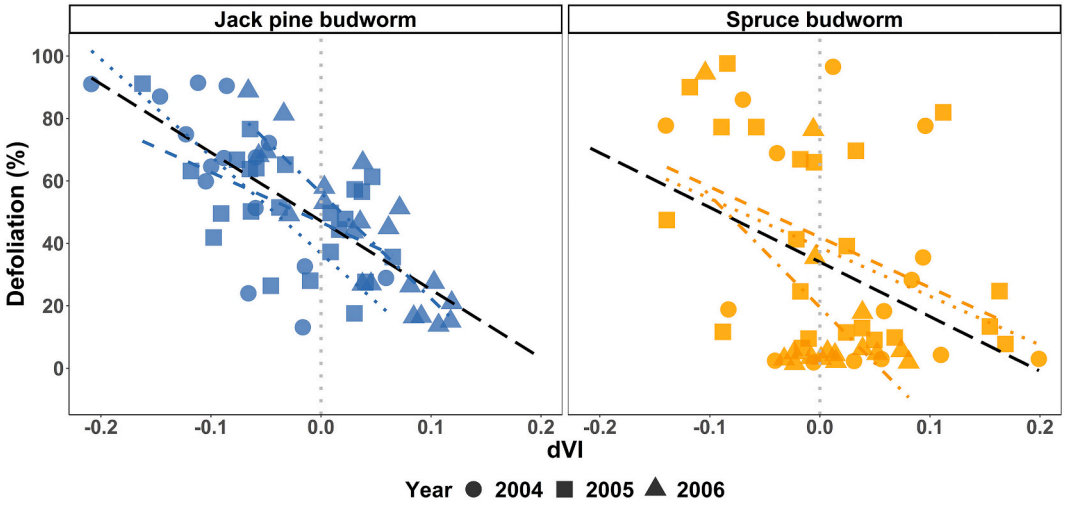

Fig. 2. Scatter plots of annual current-year defoliation with respect to the annual difference in vegetation index (dVI, more specifically difference in normalized difference vegetation index (dNDVI)) for jack pine budworm (left) and spruce budworm (right). Annual dVI was calculated using pre- and post-disturbance Landsat Imagery. Defoliation data from different year and respective linear defoliation models are indicated by different shapes and lines (dotted line for 2004, dashed line for 2005 and dotdash for 2006), respectively. Black dotted lines represent the global, linear regression between annual defoliation and dVI using pooled data across all years.

Table 2
K-year cross-validation results for each budworm-specific global model (jack pine budworm, spruce budworm). Each year of data (i.e., three years per budworm system) were iteratively withheld during model development and used for validation. Here, we report the year of field data withheld during the model development and model performance metrics, which include adjusted R^2 (R^2_{adj}), cross-validation (CV) root mean squared error (RMSE), and cross-validation mean absolute error (MAE).

Defoliators	Year	R^2_{adj}	RMSE	CV_RMSE	CV_MAE
Jack pine budworm	2004	0.49	14.49	17.95	13.43
	2005	0.61	15.67	15.49	12.15
	2006	0.42	16.27	14.50	11.63
Spruce budworm	2004	0.16	29.52	32.94	27.44
	2005	0.11	31.00	31.02	25.47
	2006	0.16	30.42	33.04	31.59

4.2. Annual defoliation across SBW, JPBW and SGM

Model comparisons suggest that non-linear mixed models are best for fitting remote sensing data (i.e., dVI) to plot-level shoot-based annual defoliation estimates across the three defoliator systems (SGM, JPBW and SBW) (Appendix E, Table S5–1, Fig. 4). Our analyses revealed that sample year did not significantly affect model performance (*p*-value = 0.91). Non-linear mixed models that included weighted variance to explain system-wide heterogeneity in defoliation resulted in a fixed asymptote (a = 100%), with two different parameters (b & c, Eq. 2) for each system, and a RMSE value of 16.98% (95% CI: 13.96%–21.75%) (Table 4). Among the three models, the SBW model resulted in the highest RMSE value, followed by SGM and JPBW (RMSE = 29.30%, 16.10% and 15.50%, respectively, Table 4). Pairwise comparison of model parameters between systems revealed that parameter *b* (i.e., rate of change in defoliation with respect to dVI) was not significantly different between JPBW and SBW models (*p*-value: 0.85). However, this rate of change parameter was significantly different between the JPBW and SGM models (*p*-value: $< 1.00 \times 10^{-4}$) and between the SBW and SGM models (*p*-value: $< 4.60 \times 10^{-3}$). Similarly, the *c* parameter (i.e., midpoint of dVI at which slope is maximum) was not significantly different between the SGM and SBW models (*p*-value: 0.47) or the JPBW and SBW models (*p*-value: 0.06), but was significantly different between SGM and JPBW models (*p*-value: $< 1.00 \times 10^{-4}$). The respective rate of change in defoliation with respect to dVI parameter, *b*, for the SBW and SGM were 1.22 and two times higher compared to that for the JPBW model. In addition, second derivative analysis of our non-linear mixed models suggests that approximately 21% annual defoliation across the tree systems (i.e., SGM 21.18%, JPBW 21.12%, and SBW 21.09%) is the optimal minimum threshold for remote detection of defoliation via dVI analysis. That is, 21% canopy annual defoliation translates to dVI values of 0.12 for JPBW, 0.04 for SBW and − 0.05 for SGM. However, it is important to note that annual defoliation of 21% across the three

Table 3
Comparison of the combined budworm system models of annual defoliation. Here, pooled field data from jack pine budworm (JPBW) and spruce budworm (SBW) by year were used to develop one global budworm model. Winter normalized difference vegetation index (NDVI) imagery from pre- and post-defoliation years were used to calculate difference in vegetation index (dVI). Covariates, that include year of field data collection and budworm system, were used to test the effects on global model calibration.

Data	Model Description (JPBW + SBW)	DF	R^2_{adj}	RMSE	AIC	*p*-val
All	mod1: Defoliation ~ dVI	110	0.31	24.48	1038.13	1.40×10^{-10}
	mod2: Defoliation ~ dVI + Year	108	0.30	24.52	1040.42	3.25×10^{-9}
	mod3: Defoliation ~ dVI + Budworm	109	0.35	23.7	1031.86	2.27×10^{-11}
	mod4: Defoliation ~ dVI + Year + Budworm	107	0.35	23.62	1033.04	1.96×10^{-10}
Subset: Defoliation > 10%	mod1a: Defoliation ~ dVI	87	0.33	20.53	794.48	2.08×10^{-9}
	mod2a: Defoliation ~ dVI + Year	85	0.32	20.71	797.92	7.48×10^{-8}
	mod3a: Defoliation ~ dVI + Budworm	86	0.33	20.55	795.62	1.18×10^{-8}
	mod4a: Defoliation ~ dVI + Year + Budworm	84	0.32	20.68	798.65	1.80×10^{-7}

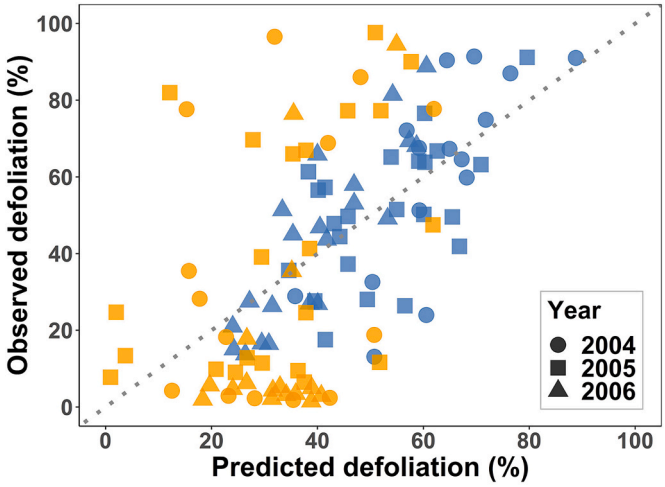

Fig. 3. Budworm global, linear regression model results for annual defoliation with respect to annual change in normalized difference in vegetation index (dNDVI) using pooled data across both budworm systems, where all blue symbols represent jack pine budworm data and all yellow symbols represent spruce budworm data. Field season years are represented by circle (2004), square (2005) and triangle (2006). Gray dotted line represents 1:1 correspondence. (For interpretation of the references to colour in this figure legend, the reader is referred to the web version of this article).

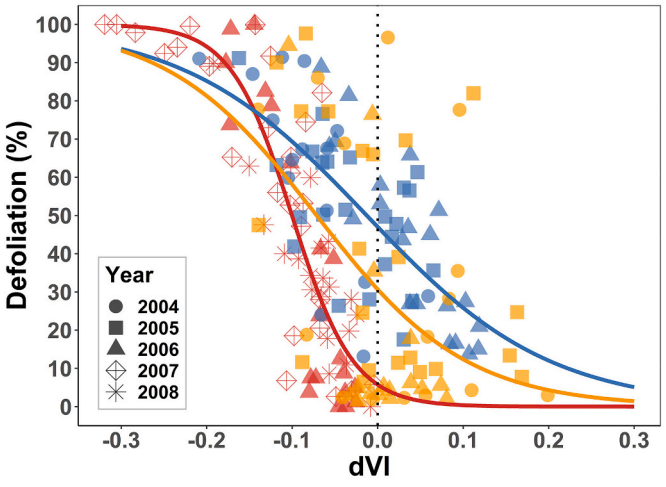

Fig. 4. Non-linear mixed models for annual difference in Landsat-based vegetation indices (dVI) with respect to annual defoliation for three different defoliators: spruce budworm (yellow symbols), jack pine budworm (blue symbols), and spongy moth (red symbols). Normalized difference vegetation index (NDVI) images, calculated from winter imagery, were used for both budworm systems (spruce budworm and jack pine budworm), while normalized difference infrared index (NDII) imagery, derived from the growing season, were used for the spongy moth system to calculate dVI. The three colored lines represent the best non-linear mixed model fits for each, respective, defoliator system. Different shapes of symbol represent the year of defoliation field data collection. (For interpretation of the references to colour in this figure legend, the reader is referred to the web version of this article).

systems does not necessarily translate to same amount of foliage biomass loss (see Jenkins et al., 2003).

4.3. Ecosystem defoliation metrics for SGM and JPBW

We found a non-linear mixed model with two different parameters (a, and c, Eq. 2) for each system was optimal when cumulative annual frass data from two systems (SGM and JPBW) were combined (Appendix E, Table S5–2, Fig. 5). The optimal model in this case included weighted residual variance to account for system-wide heterogeneity in the frass data, which resulted in an RMSE of 4.75 kg·ha^{-1} (95% CI: 0.58, 14.69) (Table 5). We found that the rates of change in dVI values (parameter *b*) were not significantly different (*p*-value = 0.46) between these two systems but the parameter *c* was significantly different (*p*-value $<1.00 \times 10^{-4}$). The estimated asymptote values, parameter *a*, for SGM and JPBW were 1970.52 kg·ha^{-1} and 649.93 kg·ha^{-1}, respectively (Table 5). Again, second derivative analysis of the models suggests that critical dVI values, where change in dVI to frass deposition were distinct, were −0.02 for SGM and 0.14 for JPBW. As such, the optimal minimum frass deposition values detected via dVI analysis were 417.76 kg·ha^{-1} and 137.67 kg·ha^{-1} for SGM and JPBW, respectively.

Similar to the comparisons for pooled frass biomass above, we found that a non-linear mixed model with two separate parameters (*a* and *c*, Eq. 2) for each system was optimal for the combined foliage loss data

Table 4
Non-linear mixed model parameters for annual defoliation across the three systems: spongy moth (SGM), jack pine budworm (JPBW) and spruce budworm (SBW). The 95% confidence interval (CI) for slope (b) and scale (c) parameters are given in bracket. Model performance metrics include root mean squared error (RMSE) and mean squared error (MSE).

Defoliators	Parameters (95% CI)		RMSE (%)	MSE (%)
	b	c		
Spongy moth	27.93 (20.69, 35.16)	−0.10 (−0.10, −0.09)	16.14 (12.78, 19.71)	12.57 (10.62, 13.85)
Jack pine budworm	9.34 (−5.62, 24.31)	−0.01 (−0.04, 0.01)	15.45 (13.53, 17.84)	12.35 (11.19, 13.59)
Spruce budworm	11.42 (−5.98, 28.82)	−0.07 (−0.12, −0.01)	29.25 (26.07, 32.83)	24.40 (23.34, 26.18)

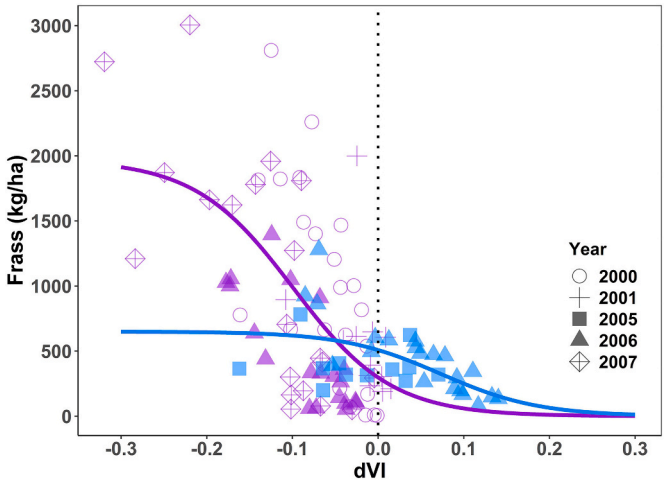

Fig. 5. Non-linear mixed model results for seasonal, cumulative frass (kg/ha) with the annual change in vegetation index (dVI) for spongy moth (purple) and jack pine budworm (blue). Seasonal cumulative frass biomass was calculated by adding daily frass rate (kg/ha) over the feeding season for each year. Normalized difference vegetation index (NDVI) images, calculated from winter imagery, was used for jack pine budworm system, while normalized difference infrared index (NDII) imagery, derived from the growing season, were used for the spongy moth system to calculate dVI. The colored lines represent the best non-linear mixed model fits for each, respective, defoliator system. Different shapes of symbol represent the year of defoliation field data collection. (For interpretation of the references to colour in this figure legend, the reader is referred to the web version of this article).

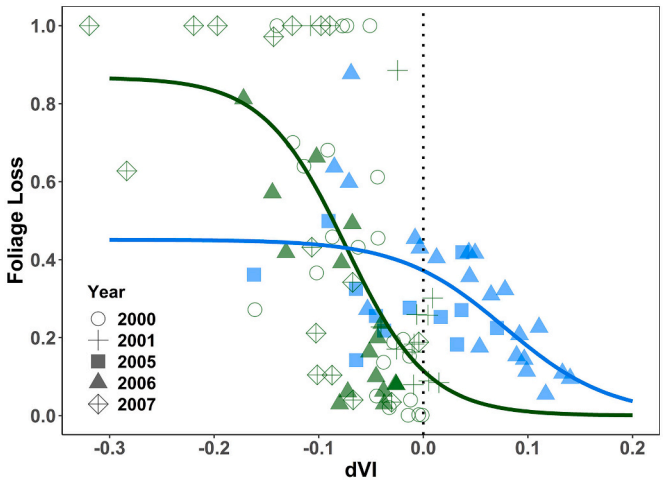

Fig. 6. Non-linear mixed model results for foliage loss with respect to annual change in vegetation index (dVI) for spongy moth (green) and jack pine budworm (blue). Foliage loss is the proportion of biomass loss (eaten plus green fall) by respective defoliator to total amount of foliage biomass available. Normalized difference vegetation index (NDVI) images, calculated from winter imagery, was used for jack pine budworm system, while normalized difference infrared index (NDII) imagery, derived from the growing season, were used for the spongy moth system to calculate dVI. The colored lines represent the best non-linear mixed model fits for each, respective, defoliator system. Different shapes of symbol represent the year of defoliation field data collection. (For interpretation of the references to colour in this figure legend, the reader is referred to the web version of this article).

Table 5
Non-linear mixed model parameters for frass biomass across the two systems: spongy moth and jack pine budworm. The 95% confidence interval (CI) for slope (b) and scale (c) parameters are given in bracket. Model performance metrics include root mean squared error (RMSE) and mean squared error (MSE).

Defoliators	Parameters (95% CI)		RMSE ($kg \cdot ha^{-1}$)	MSE ($kg \cdot ha^{-1}$)
	a	c		
Spongy moth	1970.52 (804.99, 3136.16)	−0.09 (−0.17, −0.02)	561.60 (471.75, 667.63)	435.98 (249.19, 548.85)
Jack pine budworm	649.93 (−1612.26, 2912.13)	0.07 (−0.07, 0.22)	205.43 (199.85, 211.00)	164.51 (141.76, 187.26)

b: 17.41 (7.78, 27.05).

Table 6
Non-linear mixed model parameters for proportion of foliage loss across the two systems: spongy moth and jack pine budworm. The 95% confidence interval (CI) for slope (b) and scale (c) parameters are given in bracket. Model performance metrics include root mean squared error (RMSE) and mean squared error (MSE).

Defoliators	Parameters		RMSE	MSE
	a	c		
Spongy moth	0.88 (0.62, 1.13)	−0.07 (−0.10, −0.04)	0.37 (0.24, 0.49)	0.29 (0.19, 0.41)
Jack pine budworm	0.43 (−0.07, 0.93)	0.08 (5.00×10^{-3}, 0.16)	0.19 (0.12, 0.26)	0.15 (0.10, 0.21)

b: 24.31 (11.73, 36.90).

(JPBW and SGM), which includes the weighted variance to account for heterogeneity in the foliage loss data (Appendix E, Table S5–3, Fig. 6). The RMSE value from the optimal foliage loss model was 0.26% with a 95% CI of 0.20% to 0.30%. Between the two systems, we found significant differences in foliage loss asymptote values (0.88 for SGM vs 0.43 for JPBW, p-value $= 6.00 \times 10^{-4}$, Table 6) and dVI values associated with maximum slope (−0.07 for SGM vs 0.08 for JPBW, p-value $\leq 1.00 \times 10^{-4}$, Table 6). However, the rate of change in dVI with respect to foliage loss was not significantly different between SGM and JPBW systems (p-value $= 0.67$). Nevertheless, we used the second derivative to identify the dVI values −0.02 for SGM and 0.13 for JPBW, at which foliage loss (threshold values 0.18 and 0.09 for SGM and JPBW, respectively) was remotely discernable.

5. Discussion

5.1. Annual defoliation in conifer

We examined the relationship between continuous levels of coniferous budworm defoliation and the associated changes in NDVI difference image values (i.e., dNDVI) calculated using winter Landsat sensor data. In the case of SBW, it is important to recognize that forest composition in the mixed Laurentian forests of the Great Lakes region contrast strongly with those of eastern maritime systems, where much previous work has been reported, and where the density and canopy dominance of spruce-fir host is often substantially greater (Rahimzadeh-Bajgiran et al., 2018). In contrast, jack pine clearly dominates the JPBW system with respect to both concentration and canopy position in Wisconsin's Northwest Sands Ecoregion (Wisconsin Department of Natural Resources, 2015). Given this, the combined budworm (SBW and JPBW) annual defoliation model (i.e., global model) performed poorly in terms of the adjusted coefficient of determination statistic ($R^2_{adj} = 0.35$). However, the resulting RMSE value (23.70%) was superior to that reported for similar, but thematic mapping efforts conducted with early July Sentinel-2 satellite sensor data within SBW systems in the eastern Maritimes (32% RMSE, Bhattarai et al., 2020). This is notable, because they tested several indices that incorporate data from the three Sentinel-2 red-edge bands (20-m pixels), a region of the electromagnetic spectrum noted for increased sensitivity to forest canopy damage (Rock et al., 1988). Also working in eastern Maritimes, (Rahimzadeh-Bajgiran

et al., 2018) reported similar annual SBW defoliation mapping results, where the authors used BioSIM to target peak SBW larval feeding phenology as a means to select optimal Landsat imagery for capturing the red-attack windows of opportunity each year. Given this image selection strategy, they were able to map three classes of SBW defoliation (light, moderate, and heavy) to 60%, 52%, and 77% accuracy, respectively. Overall, they achieved a 32% classification error among all annual SBW defoliation levels. Interestingly, the use of Hyperion satellite sensor data in a recent annual SBW defoliation study (Donovan et al., 2021) did not substantially improve overall classification accuracy compared to other studies (64%), where the moderate defoliation class (30%–70%) had the highest level of confusion with other classes. In other conifer defoliation studies, the use of vegetation change indices derived from Sentinel-2 data and support vector regression (SVR) yielded a moderate cumulative defoliation model (R^2 = 0.57 and RMSE = 11.6%) among natural *Pinus sylvestris* L. stands (Hawryło et al., 2018). Improved model performance metrics (R^2: 0.87–0.92 and RMSE: 0.15%–10%) are reported for other studies where numerous Landsat data stacks or high spatial resolution multispectral imagery are used to quantify cumulative defoliation (Leckie et al., 1992; Zhu et al., 2018). In contrast, we modeled annual budworm defoliation leveraging consecutive annual changes in NDVI through time calculated using archived winter Landsat sensor data. Specifically, we showed that it is possible to model budworm defoliation within a relatively homogenous coniferous host system (JPBW) with moderate overall average precision (R^2_{adj} = 0.52, RMSE = 15.44%) to levels similar to that reported by Hawryło et al. (2018). Our best defoliation model performance was our 2006 continuous annual JPBW model, with an R^2_{adj} of 0.75 and RMSE of 11.29%.

As we expected, continuous models of JPBW annual defoliation outperformed SBW annual defoliation models. Our results explain, in part, the strong differences in forest compositional complexity and differences in budworm defoliation dynamics between the two systems. Two dominant factors affected the budworm-defoliated host's optical characteristics and the resulting change in NDVI values: (1) homogenous distribution of host (both horizontally and vertically) and (2) the distribution of foliage age. Specifically, 100% annual defoliation in JPBW systems means only partial consumption of the total live foliar biomass because jack pine trees, on average, retain roughly two years of foliage, of which only the current-year's foliage is palatable (Radeloff et al., 1999a). However, in SBW systems a similarly severe defoliation translates to consumption of ca. 28% of total live foliage biomass, as host species may retain up to six years of foliage (MacLean et al., 2001). Despite this, ancillary data on forest structure and composition did not explain system differences in our ability to map defoliation, indicating that further effort is required to understand the influence of forest and ecosystem complexity on defoliation detection.

The severity of defoliation in any given year is a function of caterpillar density and remaining host availability (Nealis and Régnière, 2004). As such, we observed variable or deceasing annual defoliation in successive defoliation years (i.e., 2004 to 2006) within each budworm system (SBW: 34.9%, 41.14%, and 12.77%; JPBW: 61.05%, 49.01%, and 43.36%). Similar to JPBW, a multi-year SBW outbreak cycle reported by Maclean and Ostaff (1989) and Nealis and Régnière (2004) had a decreasing trend in where annual defoliation decreased in successive years following the cycle's peak year. Moreover, we suspect the heavy JPBW defoliation in 2004 likely induced a reduction in pollen production in following year (Nealis et al., 2003; Nealis and Lomic, 1994), which induced the dispersal of caterpillars in search of food that resulted in relatively diffuse defoliation (Nealis et al., 2003; Nealis and Régnière, 2004). However, the ability of conifer systems to recover in the months following a relatively diffuse defoliation (Cooke et al., 2021; Nealis et al., 2003; Nealis and Régnière, 2004) may cause both a decrease in the apparent defoliation amount and an increase in current-year foliage in budworm systems. Such mechanisms could partially explain the poor 2005 JPBW annual defoliation model performance (R^2_{adj} = 0.27, RMSE = 14.93%) and positive changes in NDVI in both JPBW and SBW systems in 2006. Interestingly, Rahimzadeh-Bajgiran et al. (2018) reported similar variations in defoliation model performance following the peak disturbance year, where model accuracies decreased from 72% (2008) to 64% (2009).

We successfully demonstrated the utility of mapping annual budworm defoliation via the use of multi-temporal winter Landsat sensor data. Here, our approach to modeling budworm defoliation does not require that the pre-disturbance image year is completely free of insect disturbance, as we evaluated relative change in defoliation status from year to year. This is possible in coniferous systems, especially in our study because (1) annual defoliation in these systems refers to the percent reduction of current-year foliage and (2) because conifers, for all practical purposes, do not re-foliate during the remaining growing season following the annual defoliation. Our method of employing winter imagery to model annual defoliation circumvents two key limitations that characterize previous studies: (1) the need to capture the time-variable peak of annual defoliation (red-needle or red-attack stage) and (2) the dampening optical effects associated with summer broadleaf tree cover in mixed stand. Hence, we believe our budworm disturbance modeling approach could be easily adapted to other temperate regions where coniferous host distribution is relatively concentrated.

5.2. Defoliation detection across systems

Until now, the application of satellite remote sensing data for mapping insect defoliation has been largely system-specific and categorical in application (e.g., defoliated vs. non-defoliated). Here, we combined annual defoliation data from three different systems (SGM, JPBW, and SBW) with each system exhibiting high, moderate and low gradients of insect disturbance severity. As such, our results demonstrate that the magnitude of change expressed in Landsat-based vegetation indices, VIs, associated with defoliation is different between conifer and broadleaved systems (Figs. 5–7). For instance, 10% annual defoliation translates to a negative change in VI values for SGM (−0.02) and a positive change in VI values among the budworm systems (0.22 for JPBW and 0.12 for SBW) (Fig. 5). We suspect various factors influence the Landsat-based VI differences observed between these two broad systems. First, species-specific foliar reflectance in the NIR region (0.77–0.9 um) is more sensitive to disturbance change in broadleaf foliage compared to conifer foliage (Boresjö, 1989; Leckie, 1987; Ollinger, 2011; Vogelmann and Rock, 1988, 1989) as discussed in previous section. For instance, as in our study, Radeloff et al. (1999a) observed a positive relationship between NIR and defoliation in jack pine. These authors speculate that as the overstory is consumed the NIR contributions of the coniferous understory increase. Second, fundamental difference in shoot-defoliation assessment between conifer and broadleaf systems exist. For instance, 10% annual defoliation in a conifer system implies removal of 10% of the current-year foliage, which implies that this 90% of the current-year foliage remaining is a net increase to the total live foliage, which include multiple years of live foliage (sensu Hall et al., 2016). In contrast, 10% defoliation in a broadleaf system is a net foliage loss, as there is only one year of foliage in any given year. Moreover, optical dampening resulting from the presence of broadleaved trees in mixed conifer stands, as in our case (Ekstrand, 1994; Leckie, 1987; Rock et al., 1988).

For budworm systems, a negative change in NDVI is typically associated with >70% annual budworm defoliation. However, a high level of defoliation (>70%) in a budworm system is considered moderate defoliation when compared to a SGM system. As we explained earlier, quantifying annual defoliation among conifer and broad-leaf defoliator systems differs dramatically due to differences in foliage retention and longevity. That is, annual defoliation in SBW and JPBW refers primarily to the loss of current-year foliage among multiple years of unpalatable live foliage retained, while similar levels of SGM defoliation refers to total loss all foliage. Hence, 70% annual defoliation in SGM translates to 35% of JPBW (*per. Observation,*(O'Neil, 1962)) and 20% of SBW (MacLean et al., 2001) defoliation when scaled to total amount of live

foliage. In this context, the maximum canopy defoliation (frass and foliage loss) in JPBW system is equivalent to 40% defoliation in SGM (Figs. 5-6). Scaling of canopy defoliation to same units (frass [kg·ha^{-1}] and foliage loss [0–1]) enables cross-system comparisons with respect to dVI (Figs. 5-6).

To our knowledge, this study is the first to show the clear association between dVI values and foliage loss, as well as frass deposition across multiple defoliator systems. Our study shows that defoliation models for conifer and broadleaved systems perform best when separated, especially when the aim is to estimate low levels of defoliation. It is important to note that the performance of a predictive defoliation model can be improved at the individual tree level when hyperspectral sensor data are combined with LiDAR sensor data ($R^2 = 0.81$ and RMSE = 14.46%, Meng et al., 2018). While such approaches may not yet be feasible for regional mapping purposes due to the lack of multi-temporal LiDAR, higher spatial and spectral resolution imagery combined with novel approaches will likely further improve model performance (Lottering et al., 2019; Lottering and Mutanga, 2016) to support regional mapping needs in the future.

6. Conclusion

We present a comprehensive study of budworm defoliation detection in primarily coniferous systems (SBW and JPBW) and compare these results to those of a broadleaf system (SGM) through the analysis of ground-to-satellite calibrated defoliation models across the three systems. We found that the magnitude and direction of change in Landsat-based vegetation index values, VIs, due to defoliation are substantially different in terms of biological meaning between budworm and broadleaf defoliator systems. That is, one unit of change in VI difference, dVI, translates to different amount of foliar biomass among systems, which precludes the development of one global defoliation model. As such, we recommend using separate, system-specific models to capture the difference in system-specific biological impacts, especially for coniferous and broadleaf systems. With respect to budworm systems, our analyses show that NDVI change imagery, calculated using winter Landsat sensor data, provides a robust and appropriate approach for modeling and mapping annual defoliation in conifer systems. Particularly among homogenous conifer stands, when continuous defoliation mapping is the goal, the method describe here provides a simple way to estimate annual defoliation when either copious clouds or poor sensor overpass timing precludes capture of the optimal window of opportunity for peak defoliation detection in summer. This paper contributes to the ensemble learning of canopy defoliation by using three different approaches to measure canopy defoliation: shoot-based estimates (%), frass biomass (kg·ha^{-1}), and foliage loss derived from frass which can be used to assess annual forest health, nutrient flux and carbon dynamics, respectively. We believe both the inclusion of defoliator population dynamics in disturbance assessments and use of hyperspectral sensor data will likely lead to advancements in the detection and mapping of continuous defoliation in future.

Authors contributions

- B.T., P.W., B.S., and P.T. conceived and designed research and interpreted results.
- B.T. wrote initial manuscript and led data analysis.
- B.S. and P.T. led the field campaigns in Minnesota, Wisconsin, and Maryland.
- All authors read and edited all versions of this manuscript.

Declaration of Competing Interest

The authors declare that they have no known competing financial interests or personal relationships that could have appeared to influence the work reported in this paper.

Data availability

Data will be made available on request.

Acknowledgments

We would like to thank all the following institutions for their financial support (Department of Natural Resource Ecology and Management, Iowa State University, Ames, IA 50011; USDA McIntire Stennis Capacity Grant IOW5348 [P.T. Wolter]; USDA Forest Service Northern Research Station; USDA Forest Service joint venture grant [15-JV-11242313-089]; USDA Forest Service, Forest Health Monitoring and Evaluation Monitoring grant [BRS and PAT]; NASA Carbon Cycling Program grant NNX06AD45G [PAT and BRS]; Northeastern States Research Cooperative award [BRS]; and the US Endowment for Forest and Communities project [E2014-0260]). We would also like to thank the following individuals that contributed to the study design and field data collection: Shane Weber, Bill Mattson, Jamie Walter, Nate Aspelin, Brian Miranda, Clayton Kingdon, Partick James, Rob Scheller, Jeff Griffith, Randy Richardson (RIP), Ben Townsend, Cindee Giffen, Chris Welcker, Jeremiah Sawma, Robert Chastain, Keith Lott, Clay Baros, Wendy Hunter, Michael Snyder, James Morgan. We would like to acknowledge the original project investigators Keith Eshleman and Steven Seagle for spongy moth studies in Maryland and David Mladenoff for both jack pine budworm and spongy moth studies in Wisconsin and Maryland, respectively. In addition, we would like to thank Dr. David A. Orwig for suggestions and comments on the manuscript. Finally, we would like to extent our sincere thanks to the anonymous reviewers for valuable suggestions to improve the clarity and presentation of this manuscript. The conclusions and opinions in this paper are those of the authors and not of the all the institutions and individuals who supported this work through funding and field work.

Appendix A. Supplementary data

Supplementary data to this article can be found online at https://doi.org/10.1016/j.rse.2022.113236.

References

Amos-Binks, L.J., MacLean, D.A., Wilson, J.S., Wagner, R.G., 2010. Temporal changes in species composition of mixedwood stands in northwest New Brunswick: 1946-2008. Can. J. For. Res. 40, 1–12. https://doi.org/10.1139/X09-162.

Barbosa, P., Greenblatt, J., 1979. Suitability, digestibility and assimilation of various host plants of the gypsy moth Lymantria dispar L. Oecologia, 1979, 431 (43), 111–119. https://doi.org/10.1007/BF00346676.

Batzer, H.O., Hastings, A.R., 1981. Rating spruce-fir stands for spruce budworm vulnerability in Minnesota, pp. 105–108.

Bhattarai, R., Rahimzadeh-Bajgiran, P., Weiskittel, A., MacLean, D.A., 2020. Sentinel-2 based prediction of spruce budworm defoliation using red-edge spectral vegetation indices. Remote Sens. Lett. 11, 777–786. https://doi.org/10.1080/2150704X.2020.1767824.

Boresjö, L., 1989. Landsat Tm and Spot data for medium-scale mapping of swedish vegetation types. Report, 3571.

Breiman, L., 2001. Randomn forests. In: Machine learning, 45. Kluwer Academic Publishers. Manufactured in The, Netherlands, pp. 5–32.

Burnham, K., Inference, D.A., 2002. A practical information-theoretic approach. Model Sel. multimodel inference 2.

Carisey, N., Bauce, E., 1997. Impact of balsam fir flowering on pollen and foliage biochemistry in relation to spruce budworm growth, development and food utilization. Entomol. Exp. Appl. 85, 17–31. https://doi.org/10.1046/J.1570-7458.1997.00231.X.

Castagneyrol, B., Jactel, H., Vacher, C., Brockerhoff, E.G., Koricheva, J., 2014. Effects of plant phylogenetic diversity on herbivory depend on herbivore specialization. J. Appl. Ecol. 51, 134–141. https://doi.org/10.1111/1365-2664.12175.

Chen, C., Weiskittel, A., Bataineh, M., MacLean, D.A., 2017. Evaluating the influence of varying levels of spruce budworm defoliation on annualized individual tree growth and mortality in Maine, USA and New Brunswick, Canada. For. Ecol. Manag. 396, 184–194. https://doi.org/10.1016/j.foreco.2017.03.026.

Christenson, L.M., Lovett, G.M., Mitchell, M.J., Groffman, P.M., 2002. The fate of nitrogen in gypsy moth frass deposited to an oak forest floor. Oecologia 131, 444–452. https://doi.org/10.1007/s00442-002-0887-7.

Clancy, K.M., Giese, R.L., Benjamin, D.M., 1980. Predicting Jack-pine budworm infestations in northwestern Wisconsin1. Environ. Entomol. 9, 743–751. https://doi.org/10.1093/ee/9.6.743.
Clark, J., 1961. Photosynthesis and respiration in white spruce and balsam fir. NY State coll. Forest. Techn. Pub 85.
Claverie, M., Vermote, E.F., Franch, B., Masek, J.G., 2015. Evaluation of the Landsat-5 TM and Landsat-7 ETM+ surface reflectance products. Remote Sens. Environ. 169, 390–403. https://doi.org/10.1016/j.rse.2015.08.030.
Cooke, B.J., Nealis, V.G., Régnière, J., 2021. Insect defoliators as periodic disturbances in northern forest ecosystems. In: Plant Disturbance Ecology. Elsevier, pp. 423–461. https://doi.org/10.1016/b978-0-12-818813-2.00012-5.
Coppin, P., Jonckheere, I., Nackaerts, K., Muys, B., Lambin, E., 2004. Digital change detection methods in ecosystem monitoring: a review. Int. J. Remote Sens. 25, 1565–1596. https://doi.org/10.1080/0143116031000101675.
Dale, Joyce, McNulty, Neilson, Ayres, Flannigan, Hanson, Irland, Lugo, Peterson, Simberloff, Swanson, Stocks, Wotton, 2001. Climate Change and Forest Disturbances | BioScience | Oxford Academic. https://academic.oup.com/bioscience/article/51/9/723/288247 (accessed 8.21.21).
de Beurs, K.M., Townsend, P.A., 2008. Estimating the effect of gypsy moth defoliation using MODIS. Remote Sens. Environ. 112, 3983–3990. https://doi.org/10.1016/j.rse.2008.07.008.
Donovan, S.D., MacLean, D.A., Zhang, Y., Lavigne, M.B., Kershaw, J.A., 2021. Evaluating annual spruce budworm defoliation using change detection of vegetation indices calculated from satellite hyperspectral imagery. Remote Sens. Environ. 253 https://doi.org/10.1016/j.rse.2020.112204.
Dymond, C.C., Neilson, E.T., Stinson, G., Porter, K., MacLean, D.A., Gray, D.R., Campagna, M., Kurz, W.A., 2010. Future spruce budworm outbreak may create a carbon source in eastern Canadian forests. Ecosystems 13, 917–931. https://doi.org/10.1007/s10021-010-9364-z.
Ekstrand, S.P., 1990. Detection of moderate damage on Norway spruce using Landsat TM and digital stand data. IEEE Trans. Geosci. Remote Sens. 28, 685–692. https://doi.org/10.1109/TGRS.1990.572982.
Ekstrand, S., 1994. Assessment of forest damage with landsat TM: correction for varying forest stand characteristics. Remote Sens. Environ. 47, 291–302. https://doi.org/10.1016/0034-4257(94)90097-3.
Fettes, J., 1950. Investigation of sampling techniques for population studies of the spruce budworm on balsam fir in Ontario. For. Insect Lab, Sault Ste Marie, Ont. Annu Tech Rep 4.
Fleming, R.A., Piene, H., 1992. Spruce budworm defoliation and growth loss in young balsam fir: period models of needle survivorship for spaced trees. For. Sci. 38, 287–304. https://doi.org/10.1093/forestscience/42.3.282.
Fleming, R.A., Candau, J.N., McAlpine, R.S., 2002. Landscape-scale analysis of interactions between insect defoliation and forest fire in central Canada. Clim. Chang. 55, 251–272. https://doi.org/10.1023/A:1020299422491.
Foster, J.R., 2017. Xylem traits, leaf longevity and growth phenology predict growth and mortality response to defoliation in northern temperate forests. Tree Physiol. 37, 1151–1165. https://doi.org/10.1093/treephys/tpx043.
Franklin, J.F., Spies, T.A., Van Pelt, R., Carey, A.B., Thornburgh, D.A., Berg, D.R., Lindenmayer, D.B., Harmon, M.E., Keeton, W.S., Shaw, D.C., Bible, K., Chen, J., 2002. Disturbances and structural development of natural forest ecosystems with silvicultural implications, using Douglas-fir forests as an example. For. Ecol. Manag. 155, 399–423. https://doi.org/10.1016/S0378-1127(01)00575-8.
Franklin, S.E., Fan, H., Guo, X., 2008. Relationship between landsat TM and SPOT vegetation indices and cumulative spruce budworm defoliation. Int. J. Remote Sens. 29, 1215–1220. https://doi.org/10.1080/01431160701730136.
Frelich, L.E., 2002. Forest Dynamics and Disturbance Regimes: Studies from Temperate Evergreen-Deciduous Forests. Cambridge Univ. Press.
Goodfellow, I., Bengio, Y., Courville, A., 2017. Deep Learning - Adaptive Computation and Machine Learning. MIT Press, Massachusetts, USA.
Hall, R.J., Volney, W.J.A., Wang, Y., 1998. Using a geographic information system (GIS) to associate forest stand characteristics with top kill due to defoliation by the jack pine budworm. Can. J. For. Res. 28, 1317–1327. https://doi.org/10.1139/X98-108.
Hall, R.J., Fernandes, R.A., Hogg, E.H., Brandt, J.P., Butson, C., Case, B.S., Leblanc, S.G., 2003. Relating aspen defoliation to changes in leaf area derived from field and satellite remote sensing data. Can. J. Remote. Sens. 29, 299–313. https://doi.org/10.5589/m03-001.
Hall, R.J., Castilla, G., White, J.C., Cooke, B.J., Skakun, R.S., 2016. Remote sensing of forest pest damage: a review and lessons learned from a Canadian perspective. Can. Entomol. 148, S296–S356. https://doi.org/10.4039/tce.2016.11.
Hawryło, P., Bednarz, B., Wężyk, P., Szostak, M., 2018. Estimating defoliation of scots pine stands using machine learning methods and vegetation indices of Sentinel-2. Eur. J. Remote Sens. 51, 194–204. https://doi.org/10.1080/22797254.2017.1417745.
Hicke, J.A., Allen, C.D., Desai, A.R., Dietze, M.C., Hall, R.J., Hogg, E.H. (Ted), Kashian, D.M., Moore, D., Raffa, K.F., Sturrock, R.N., Vogelmann, J., 2012. Effects of biotic disturbances on forest carbon cycling in the United States and Canada. Glob. Chang. Biol. 18, 7–34. https://doi.org/10.1111/J.1365-2486.2011.02543.X.
Host, G.E., White, M.A., 2003. Contemporary forest composition and spatial patterns of north central and northeastern Minnesota: an assessment using 1990s Landsat data, mn.gov.
Howse, G.M., 1983. Insect pests of jack pine: biology, damage, and control. In: Proceedings: Jack Pine Symposium. October 18–20, 1983, Timmins, Ontario.
Irland, L., McWilliams, W.H., 2014. Spruce budworm returns to the northeast. Northern Logger 63 (4), 10–12.
Jenkins, J.C., Chojnacky, D.C., Heath, L.S., Birdsey, R.A., 2003. National-scale biomass estimators for United States tree species. For. Sci. 49, 12–35. https://doi.org/10.1093/forestscience/49.1.12.
Karel, T.H., Man, M., 2017. Major Forest Insect and Disease Conditions in the United States: 2015. Forest Service (FS)-1093.
Kennedy, R.E., Yang, Z., Cohen, W.B., 2010. Detecting trends in forest disturbance and recovery using yearly Landsat time series: 1. LandTrendr - temporal segmentation algorithms. Remote Sens. Environ. 114, 2897–2910. https://doi.org/10.1016/j.rse.2010.07.008.
Kulman, H., Hodson, A., Duncan, D., 1963. Distribution and effects of Jack-pine budworm defoliation. For. Sci. 9, 146–157. https://doi.org/10.1093/forestscience/9.2.146.
Leckie, D.G., 1987. Factors affecting defoliation assessment using airborne multispectral scanner data (Canada). Photogramm. Eng. Remote. Sens. 53, 1665–1674.
Leckie, D.G., Ostaff, D.P., 1988. Classification of airborne multispectral scanner data for mapping current defoliation caused by the spruce budworm. For. Sci. 34, 259–275. https://doi.org/10.1093/forestscience/34.2.259.
Leckie, D.G., Teillet, P.M., Ostaff, D.P., Fedosejevs, G., 1988. Sensor band selection for detecting current defoliation caused by the spruce budworm. Remote Sens. Environ. 26 https://doi.org/10.1016/0034-4257(88)90118-6.
Leckie, D.G., Yuan, X., Ostaff, D.P., Piene, H., MacLean, D.A., 1992. Analysis of high resolution multispectral MEIS imagery for spruce budworm damage assessment on a single tree basis. Remote Sens. Environ. 40, 125–136. https://doi.org/10.1016/0034-4257(92)90010-H.
Lottering, R., Mutanga, O., 2016. Optimising the spatial resolution of WorldView-2 pan-sharpened imagery for predicting levels of Gonipterus scutellatus defoliation in KwaZulu-Natal, South Africa. ISPRS J. Photogramm. Remote Sens. 112, 13–22. https://doi.org/10.1016/j.isprsjprs.2015.11.010.
Lottering, R., Mutanga, O., Peerbhay, K., Ismail, R., 2019. Detecting and mapping Gonipterus scutellatus induced vegetation defoliation using WorldView-2 pan-sharpened image texture combinations and an artificial neural network. J. Appl. Remote. Sens. 13, 1. https://doi.org/10.1117/1.jrs.13.014513.
MacLean, D.A., 1980. Vulnerability of fir-spruce stands during uncontrolled spruce budworm outbreaks: a review and discussion. For. Chron. 56, 213–221. https://doi.org/10.5558/tfc56213-5.
MacLean, D.A., MacKinnon, W.E., 1998. Sample sizes required to estimate defoliation of spruce and balsam fir caused by spruce budworm accurately. North. J. Appl. For. 15, 135–140. https://doi.org/10.1093/njaf/15.3.135.
Maclean, D.A., Ostaff, D.P., 1989. Patterns of balsam fir mortality caused by an uncontrolled spruce budworm outbreak. Can. J. For. Res. 19, 1087–1095. https://doi.org/10.1139/x89-165.
MacLean, D.A., Piene, H., 1995. Spatial and temporal patterns of balsam fir mortality in spaced and unspaced stands caused by spruce budworm defoliation. Can. J. For. Res. 25, 902–911. https://doi.org/10.1139/x95-099.
MacLean, D.A., 1990. Impact of forest pests and fire on stand growth and timber yield: implications for forest management planning. Can. J. For. Res. 20, 391–404. https://doi.org/10.1139/x90-057.
MacLean, D.A., Erdle, T.A., MacKinnon, W.E., Porter, K.B., Beaton, K.P., Cormier, G., Morehouse, S., Budd, M., 2001. The Spruce Budworm Decision Support System: forest protection planning to sustain long-term wood supply. Can. J. For. Res. 31, 1742–1757. https://doi.org/10.1139/x01-102.
Masek, J.G., Vermote, E.F., Saleous, N.E., Wolfe, R., Hall, F.G., Huemmrich, K.F., Gao, Feng, Kutler, J., Lim, Teng-Kui, 2006. A Landsat surface reflectance dataset for North America, 1990-2000. IEEE Geoscience and Remote Sensing Lett 3 (1), 68–72. https://doi.org/10.1109/LGRS.2005.857030.
Mash, J., 1996. The Land of the Living: The Story of Maryland's Green Ridge Forest, first ed. Living History Foundation of Allegany County Maryland.
McCullough, D.G., 2000. A review of factors affecting the population dynamics of jack pine budworm (Choristoneura pinus pinus freeman). Popul. Ecol. 42, 243–256. https://doi.org/10.1007/PL00012003.
Meigs, G.W., Kennedy, R.E., Cohen, W.B., 2011. A Landsat time series approach to characterize bark beetle and defoliator impacts on tree mortality and surface fuels in conifer forests. Remote Sens. Environ. 115, 3707–3718. https://doi.org/10.1016/j.rse.2011.09.009.
Meng, R., Dennison, P.E., Zhao, F., Shendryk, I., Rickert, A., Hanavan, R.P., Cook, B.D., Serbin, S.P., 2018. Mapping canopy defoliation by herbivorous insects at the individual tree level using bi-temporal airborne imaging spectroscopy and LiDAR measurements. Remote Sens. Environ. 215, 170–183. https://doi.org/10.1016/j.rse.2018.06.008.
Nealis, V.G., Lomic, P.V., 1994. Host-plant influence on the population ecology of the jack pine budworm, Choristoneura pinus (Lepidoptera: Tortricidae). Ecol. Entomol. 19, 367–373. https://doi.org/10.1111/J.1365-2311.1994.TB00254.X.
Nealis, V.G., Régnière, J., 2004. Insect-host relationships influencing disturbance by the spruce budworm in a boreal mixedwood forest. Can. J. For. Res. 34, 1870–1882. https://doi.org/10.1139/X04-061.
Nealis, V.G., Magnussen, S., Hopkin, A.A., 2003. A lagged, density-dependent relationship between jack pine budworm Choristoneura pinus pinus and its host tree Pinus banksiana. Ecol. Entomol. 28, 183–192. https://doi.org/10.1046/j.1365-2311.2003.00502.x.
Ollinger, S.V., 2011. Sources of variability in canopy reflectance and the convergent properties of plants. Wiley Online Libr. 189, 375–394. https://doi.org/10.1111/j.1469-8137.2010.03536.x.
O'Neil, L.C., 1962. Some effects of artifical defoliation on the growth of jack pine (*Pinus banksiana* Lamb). Can. J. Bot. 40, 273–280. https://doi.org/10.1139/b62-026.

Pothier, D., Mailly, D., Tremblay, S., 2005. Predicting balsam fir growth reduction caused by spruce budworm using large-scale historical records of defoliation. Ann. For. Sci. 62, 261–267. https://doi.org/10.1051/forest:2005018.

Prebble, M.L., 1975. Spruce budworm. In: Aerial Control of Forest Insects in Canada. Department of the Environment, Ottawa, Ont.

R Core Team, 2013. https://www.R-project.org/.

Radeloff, V.C., Mladenoff, D.J., Boyce, M.S., 1999a. Detecting jack pine budworm defoliation using spectral mixture analysis: separating effects from determinants. Remote Sens. Environ. 69, 156–169. https://doi.org/10.1016/S0034-4257(99)00008-5.

Radeloff, V.C., Mladenoff, D.J., He, H.S., Boyce, M.S., 1999b. Forest landscape change in the northwestern Wisconsin Pine Barrens from pre-European settlement to the present. Can. J. For. Res. 29, 1649–1659. https://doi.org/10.1139/x99-089.

Radeloff, V.C., Mladenoff, D.J., Boyce, M.S., 2000. Effects of interacting disturbances on landscape patterns: budworm defoliation and salvage logging. Ecol. Appl. 10 (1), 233–247.

Rahimzadeh-Bajgiran, P., Weiskittel, A.R., Kneeshaw, D., MacLean, D.A., 2018. Detection of annual spruce budworm defoliation and severity classification using Landsat imagery. Forests 9. https://doi.org/10.3390/f9060357.

Reich, P.B., Rich, R.L., Lu, X., Wang, Y.-P., Oleksyn, J., 2014. Biogeographic variation in evergreen conifer needle longevity and impacts on boreal forest carbon cycle projections. Proc. Natl. Acad. Sci. 111, 13703–13708. https://doi.org/10.1073/PNAS.1216054110.

Robert, L.E., Kneeshaw, D., Sturtevant, B.R., 2012. Effects of forest management legacies on spruce budworm (Choristoneura fumiferana) outbreaks. Can. J. For. Res. 42, 463–475. https://doi.org/10.1139/X2012-005.

Robert, L.E., Sturtevant, B.R., Cooke, B.J., James, P.M.A., Fortin, M.J., Townsend, P.A., Wolter, P.T., Kneeshaw, D., 2018. Landscape host abundance and configuration regulate periodic outbreak behavior in spruce budworm Choristoneura fumiferana. Ecography (Cop). 41, 1556–1571. https://doi.org/10.1111/ecog.03553.

Rock, B.N., Hoshizaki, T., Miller, J.R., 1988. Comparison of in situ and airborne spectral measurements of the blue shift associated with forest decline. Remote Sens. Environ. 24, 109–127. https://doi.org/10.1016/0034-4257(88)90008-9.

Rosas, J., Houborg, R., McCabe, M.F., 2017. Sensitivity of Landsat 8 surface temperature estimates to atmospheric profile data: a study using MODTRAN in dryland irrigated systems. Remote Sens. 9, 988. https://doi.org/10.3390/rs9100988.

Roy, D.P., Zhang, H.K., Ju, J., Gomez-Dans, J.L., Lewis, P.E., Schaaf, C.B., Sun, Q., Li, J., Huang, H., Kovalskyy, V., 2016. A general method to normalize Landsat reflectance data to nadir BRDF adjusted reflectance. Remote Sens. Environ. 176, 255–271. https://doi.org/10.1016/j.rse.2016.01.023.

Royama, T., 1984. Population dynamics of the spruce budworm Choristoneura Fumiferana. Ecol. Monogr. 54, 429–462. https://doi.org/10.2307/1942595.

Rullán-Silva, C., Olthoff, A.E., Pando, V., Pajares, J.A., Delgado, J.A., 2015. Remote monitoring of defoliation by the beech leaf-mining weevil Rhynchaenus fagi in northern Spain. For. Ecol. Manag. 347, 200–208. https://doi.org/10.1016/j.foreco.2015.03.005.

Sakamoto, Y., Ishiguro, M., Kitagawa, G., 1986. Akaike Information Criterion Statistics. Dordrecht, Netherlands D. Reide 81, p. 26853. https://doi.org/10.2307/2983028.

Schowalter, T.D., Hargrove, W.W., Crossley, D.A., 1986. Herbivory in forested ecosystems. Annu. Rev. Entomol. 31, 177–196. https://doi.org/10.1146/annurev.en.31.010186.001141.

Senf, C., Pflugmacher, D., Wulder, M.A., Hostert, P., 2015. Characterizing spectral-temporal patterns of defoliator and bark beetle disturbances using Landsat time series. Remote Sens. Environ. 170, 166–177. https://doi.org/10.1016/j.rse.2015.09.019.

Senf, C., Seidl, R., Hostert, P., 2017. Remote sensing of forest insect disturbances: current state and future directions. Int. J. Appl. Earth Obs. Geoinf. 60, 49–60.

Sharik, T.L., Adair, W., Baker, F.A., Battaglia, M., Comfort, E.J., D'Amato, A.W., Delong, C., DeRose, R.J., Ducey, M.J., Harmon, M., Levy, L., Logan, J.A., O'Brien, J., Palik, B.J., Roberts, S.D., Rogers, P.C., Shinneman, D.J., Spies, T., Taylor, S.L., Woodall, C., Youngblood, A., 2010. Emerging themes in the ecology and Management of North American Forests. Int. J. For. Res. 2010, 1–11. https://doi.org/10.1155/2010/964260.

Shumway, D.L., Abrams, M.D., Ruffner, C.M., 2001. A 400-year history of fire and oak recruitment in an old-growth oak forest in western Maryland, U.S.a. Can. J. For. Res. 31, 1437–1443. https://doi.org/10.1139/x01-079.

Song, C., Woodcock, C.E., 2003. Monitoring Forest succession with multitemporal Landsat images: factors of uncertainty. IEEE Trans. Geosci. Remote Sens. 41, 2557–2567. https://doi.org/10.1109/TGRS.2003.818367.

Sturtevant, B.R., Seagle, S.W., 2004. Comparing estimates of forest site quality in old second-growth oak forests. For. Ecol. Manag. 191, 311–328. https://doi.org/10.1016/j.foreco.2003.12.009.

Sturtevant, B.R., Cooke, B.J., Kneeshaw, D.D., Mac Lean, D.A., 2015. Modeling insect disturbance across forested landscapes: Insights from the spruce budworm. In: Simulation Modeling of Forest Landscape Disturbances. Springer International Publishing, pp. 93–134. https://doi.org/10.1007/978-3-319-19809-5_5.

Ter-Mikaelian, M.T., Korzukhin, M.D., 1997. Biomass equations for sixty-five north American tree species. For. Ecol. Manag. 97, 1–24. https://doi.org/10.1016/S0378-1127(97)00019-4.

Thapa, B., 2021. Spatio-Temporal Characterization of Insect Defoliation through Landsat Images [Unpublished Doctoral Dissertation]. Iowa State University, Ames, Iowa.

Thapa, B., Wolter, P.T., Sturtevant, B.R., Townsend, P.A., 2020. Reconstructing past forest composition and abundance by using archived Landsat and national forest inventory data. Int. J. Remote Sens. 41, 4022–4056. https://doi.org/10.1080/01431161.2019.1711245.

Thapa, B., Wolter, P.T., Sturtevant, B.R., Foster, J., Townsend, P.A., 2022. Linking Insect Frass and Phenology to Improve Estimation of Annual Forest Defoliation. MethodX (in prep).

Townsend, P.A., Foster, J.R., Chastain, R.A., Currie, W.S., 2003. Application of imaging spectroscopy to mapping canopy nitrogen in the forest of the central Appalachian mountains using hyperion and AVIRIS. IEEE Trans. Geosci. Remote Sens. 41, 1347–1354. https://doi.org/10.1109/TGRS.2003.813205.

Townsend, P.A., Eshleman, K.N., Welcker, C., 2004. Remote sensing of gypsy moth defoliation to assess varitions in stream nitrogen concentrations. Ecol. Appl. 14, 504–516. https://doi.org/10.1890/02-5356.

Townsend, P.A., Singh, A., Foster, J.R., Rehberg, N.J., Kingdon, C.C., Eshleman, K.N., Seagle, S.W., 2012. A general Landsat model to predict canopy defoliation in broadleaf deciduous forests. Remote Sens. Environ. 119, 255–265. https://doi.org/10.1016/j.rse.2011.12.023.

Turner, M.G., Collins, S.L., Lugo, A.E., Magnuson, J.J., Scott Rupp, T., Swanson, F.J., 2003. Disturbance dynamics and ecological response: the contribution of long-term ecological research. Bioscience 53, 46–56. https://doi.org/10.1641/0006-3568(2003)053[0046:DDAERT]2.0.CO;2.

Tyndall, R.W., 2015. Restoration results for a Maryland shale barren after pignut Hickory management and a prescribed burn. Castanea 80, 77–94. https://doi.org/10.2179/14-038.

Vermote, E.F., Saleous, N.El, Justice, C.O., Kaufman, Y.J., Privette, J.L., Remer, L., Roger, J.C., Tanre, D., 1997. Atmospheric correction of visible to middle-infrared EOS-MODIS data over land surfaces: Background, operational algorithm and validation. Journal of Geophysical Research: Atmospheres 102 (D14), 17131–17141. https://doi.org/10.1029/97JD00201.

Vogelmann, J.E., Rock, B.N., 1988. Assessing forest damage in high-elevation coniferous forests in Vermont and new Hampshire using thematic mapper data. Remote Sens. Environ. 24, 227–246. https://doi.org/10.1016/0034-4257(88)90027-2.

Vogelmann, J.E., Rock, B.N., 1989. Use of Thematic Mapper Data for the Detection of Forest Damage Caused by the Pear thrips. Elsevier.

Vogl, R.J., 1964. Vegetational history of Crex meadows, a prairie savanna in northwestern Wisconsin. Am. Midl. Nat. 72, 157. https://doi.org/10.2307/2423220.

Volney, W.J.A., 1992. The distribution and estimation of jack pine budworm defoliation. Can. J. For. Res. 22, 1079–1088. https://doi.org/10.1139/x92-143.

Volney, W.J.A., Fleming, R.A., 2007. Spruce budworm (*Choristoneura spp*). biotype reactions to forest and climate characteristics. Glob. Chang. Biol. 13, 1630–1643. https://doi.org/10.1111/j.1365-2486.2007.01402.x.

Volney, W.J.A., McCullough, D.G., 1994. Jack pine budworm population behaviour in northwestern Wisconsin. Can. J. For. Res. 24, 502–510. https://doi.org/10.1139/x94-067.

Weber, S., 1995. Integrating budworm into jack pine silviculture in Northwest Wisconsin. In: Jack Pine Budworm Biology and Management. Nat. Res. Canada. Inf. Rep. NOR-X-342. Canadian Forest Service, pp. 19–24.

Wisconsin Department of Natural Resources, 2015. The ecological landscapes of Wisconsin: An assessment of ecological resources and a guide to planning sustainable management. Chapter 17, Northwest Sands Ecological Landscape. Wisconsin Department of Natural Resources, PUB-SS-1131S 2015, Madison.

Zhu, Z., Woodcock, C.E., Olofsson, P., 2012. Continuous monitoring of forest disturbance using all available Landsat imagery. Remote Sens. Environ. 122, 75–91. https://doi.org/10.1016/j.rse.2011.10.030.

Zhu, C., Zhang, X., Zhang, N., Hassan, M.A., Zhao, L., 2018. Assessing the defoliation of pine forests in a long time-series and spatiotemporal prediction of the defoliation using Landsat data. Remote Sens. 10, 360. https://doi.org/10.3390/rs10030360.